On the Numerical Solution of the Nonlinear Radiation Heat Transfer Problem in a Three-Dimensional Flow

Ammar Mushtaq[a], Meraj Mustafa[b], Tasawar Hayat[c,d], and Ahmed Alsaedi[d]

[a] Research Centre for Modeling and Simulation (RCMS), National University of Sciences and Technology (NUST), Islamabad 44000, Pakistan
[b] School of Natural Sciences (SNS), National University of Sciences and Technology (NUST), Islamabad 44000, Pakistan
[c] Department of Mathematics, Quaid-I-Azam University 45320, Islamabad 44000, Pakistan
[d] Department of Mathematics, Faculty of Science, King Abdulaziz University, P. O. Box 80257, Jeddah 21589, Saudi Arabia

Reprint requests to A. M.; E-mail: ammar.mushtaq@yahoo.com, ammar.mushtaq@rcms.nust.edu.pk

Z. Naturforsch. **69a**, 705 – 713 (2014) / DOI: 10.5560/ZNA.2014-0059
Received March 28, 2014 / revised July 28, 2014 / published online October 8, 2014

The steady laminar three-dimensional magnetohydrodynamic (MHD) boundary layer flow and heat transfer over a stretching sheet is investigated. The sheet is linearly stretched in two lateral directions. Heat transfer analysis is performed by utilizing a nonlinear radiative heat flux in Rosseland approximation for thermal radiation. Two different wall conditions, namely (i) constant wall temperature and (ii) prescribed surface temperature are considered. The developed nonlinear boundary value problems (BVPs) are solved numerically through fifth-order Runge–Kutta method using a shooting technique. To ascertain the accuracy of results the solutions are also computed by using built in function bvp4c of MATLAB. The behaviours of interesting parameters are carefully analyzed through graphs for velocity and temperature distributions. The dimensionless expressions of wall shear stress and heat transfer rate at the sheet are evaluated and discussed. It is seen that a point of inflection of the temperature function exists for sufficiently large values of wall to ambient temperature ratio. The solutions are in excellent agreement with the previous studies in a limiting sense. To our knowledge, the novel idea of nonlinear thermal radiation in three-dimensional flow is just introduced here.

Key words: Three-Dimensional Flow; Nonlinear Thermal Radiation; Bi-Directional Stretching Sheet; Shooting Method; Rosseland Approximation.

1. Introduction

The study of boundary layer flow and heat transfer due to a stretching sheet has an important bearing in various industrial and technological applications. A number of technical processes concerning polymers involve the cooling of continuous strips or filaments by drawing them through a quiescent fluid. The thin polymer sheet constitutes a continuously moving surface with a non-uniform velocity through an ambient fluid. In these cases the quality of final product largely depends on the rate of cooling which is governed by the structure of the thermal boundary layer near the moving plate/sheet. The boundary layer flow over a stationary flat plate with a uniform free stream was considered by Blasius [1]. In contrast to the Blasius problem, Sakiadis [2] studied the boundary layer flow over a continuously moving flat plate in a quiescent ambient fluid. Crane [3] was probably the first to explore the flow due to a stretching surface in an otherwise ambient fluid. Crane's idea has been extended for several other features such as viscoelasticity, magnetic field, arbitrary stretching velocity, variable wall temperature or heat flux (Gupta and Gupta [4], Chakrabarti and Gupta [5], Grubka and Bobba [6], Banks [7], Chen and Char [8], Ali [9], Pop and Na [10], Magyari and Keller [11], Liao and Pop [12], Kumari and Nath [13], Hayat et al. [14 – 16], Mustafa et al. [17, 18] Ferdows et al. [19], Beg et al. [20], Khan et al. [21], etc.). A literature survey reveals that extensive research is conducted on the steady/unsteady two-dimensional boundary layer flows over a sheet.

However the three-dimensional flows due to a bi-directional stretching sheet have been scarcely reported. Wang [22] was perhaps the first to explore Crane's problem for bi-directional flow. Lakshmisha et al. [23] discussed the unsteady three-dimensional boundary layer flow over a stretching sheet. Homotopy based analytic solutions for magnetohydrodynamic (MHD) three-dimensional flow were provided by Xu et al. [24]. In another paper, Sajid et al. [25] computed homotopy solutions for three-dimensional viscoelastic flow over a stretching sheet. Liu and Andersson [26] investigated the heat transfer over a bi-directional stretching sheet with variable thermal conditions. The combined effects of heat and mass transfer in the three-dimensional flow through a porous space have been investigated by Hayat et al. [27]. The analytic solutions for three-dimensional flows of non-Newtonian fluids over a stretching sheet have been reported by Hayat et al. [28, 29]. Liu et al. [30] reported the flow and heat transfer for three-dimensional flow over an exponentially stretching surface.

The study of radiative heat transfer flow has significant importance in manufacturing industries for the design of reliable equipment, nuclear plants, gas turbines, and various propulsion devices for aircraft, missiles, satellites, and space vehicles. Raptis and Perdikis [31] investigated the flow of a viscoelastic fluid over a porous plate with thermal radiation. Seddeek [32] and Raptis et al. [33] examined the thermal radiation effect on the boundary layer flow of an electrically conducting viscous fluid. Thermal radiation effects on the flow over a flat plate with the uniform free stream are discussed by Bataller [34]. Mixed convection flow past a vertical plate with thermal radiation was investigated by Ishak [35]. He obtained the numerical solutions for some negative values of buoyancy parameter. Bhattacharyya [36] studied the effect of thermal radiation on the MHD boundary layer flow over a time-dependent shrinking sheet with internal heat generation. Radiative heat transfer in the boundary layer flow of a nanofluid was explored by Nadeem and Haq [37]. Thermal radiation and viscous dissipation effects on the unsteady boundary layer flow of a nanofluid over a stretching sheet were presented by Khan et al. [38]. In another paper Motsumi and Makinde [39] considered the similar effects on the nanofluid flow due to a continuously moving permeable flat surface. Similarly Khan et al. [40–42] also examined radiative heat transfer effects for different problems.

Recently the idea of nonlinear radiation heat transfer is introduced by the researchers to overcome both small and large temperature differences within the boundary layer (see Pantokratoras and Fang [43], Mushtaq et al. [44], Cortell [45], and Mushtaq et al. [46]). The present paper ventures further in this regime. We have explored the effects of thermal radiation in the three-dimensional flow past a stretching sheet when the temperature function in the Rosseland approximation is not further expanded about the ambient temperature. The highly nonlinear differential systems are solved numerically by shooting method with fifth-order Runge–Kutta integration technique. The solutions are also computed by using the built in function bvp4c of MATLAB. Graphical and numerical results are presented for the velocity, temperature, skin friction coefficients, and the local Nusselt number which give interesting insights on the problem under consideration.

2. Problem Formulation

We consider the steady three-dimensional flow of an incompressible viscous fluid over a stretching sheet situated at $z = 0$. Heat transfer analysis in the presence of thermal radiation is considered. Let $U_w = ax$ and $V_w = by$ be the velocities of the stretching sheet in the x- and y-directions, respectively, where a, b are positive constants (see Fig. 1). A uniform transverse magnetic field of strength B_0 is applied in z-direction. The induced magnetic field is neglected under the assumption of small magnetic Reynolds' numbers. The boundary layer equations governing the steady three-

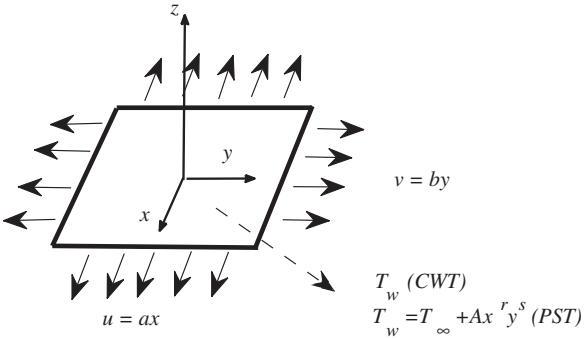

Fig. 1. Physical sketch of the problem and coordinate system.

dimensional flow are (see Sajid et al. [25] and Liu and Andersson [26])

$$\frac{\partial u}{\partial x}+\frac{\partial v}{\partial y}+\frac{\partial w}{\partial z}=0, \tag{1}$$

$$u\frac{\partial u}{\partial x}+v\frac{\partial u}{\partial y}+w\frac{\partial u}{\partial z}=\nu\frac{\partial^2 u}{\partial z^2}-\frac{\sigma B_0^2}{\rho}u, \tag{2}$$

$$u\frac{\partial v}{\partial x}+v\frac{\partial v}{\partial y}+w\frac{\partial v}{\partial z}=\nu\frac{\partial^2 v}{\partial z^2}-\frac{\sigma B_0^2}{\rho}v, \tag{3}$$

where ν is the kinematic viscosity, u, v, and w are the velocity components in the x-, y-, and z-directions, respectively.

The boundary conditions in the present problem are

$$\begin{aligned} &u=ax,\ \ v=by,\ \ w=0\ \text{ at } z=0,\\ &u=v=0\ \text{ as } z\to\infty. \end{aligned} \tag{4}$$

Using the dimensionless variables (see Wang [22])

$$\begin{aligned} &\eta=\sqrt{\frac{a}{\nu}}z,\ \ u=axf'(\eta),\\ &v=ayg'(\eta),\ \ w=-\sqrt{\nu a}(f+g), \end{aligned} \tag{5}$$

then (1) is identically satisfied, and (2)–(4) take the following forms:

$$f'''-f'^2+(f+g)f''-Mf'=0, \tag{6}$$

$$g'''-g'^2+(f+g)g''-Mg'=0, \tag{7}$$

$$\begin{aligned} &f(0)=0,\ \ g(0)=0,\ \ f'(0)=1,\ \ g'(0)=c,\\ &f'(+\infty)\to 0,\ \ g'(+\infty)\to 0, \end{aligned} \tag{8}$$

where $M=(\sigma B_0^2)/\rho a$ is the magnetic parameter, and $c=b/a$ is the velocity ratio. The quantities of practical interest, the local skin friction coefficient along x- and y-directions, are defined as

$$C_{fx}=\frac{\tau_{xz}}{\rho U_w^2};\ \ \tau_{xz}=\mu\left(\frac{\partial u}{\partial z}\right)_{z=0}, \tag{9}$$

$$C_{fy}=\frac{\tau_{yz}}{\rho V_w^2};\ \ \tau_{yz}=\mu\left(\frac{\partial v}{\partial z}\right)_{z=0}. \tag{10}$$

Using the dimensionless variables (5), we obtain

$$\mathrm{Re}_x^{1/2}C_{fx}=f''(0), \tag{11}$$

$$c^{3/2}\mathrm{Re}_y^{1/2}C_{fy}=g''(0), \tag{12}$$

where $\mathrm{Re}_x=(U_w x)/\nu$ and $\mathrm{Re}_y=(V_w y)/\nu$ are the local Reynolds number in the x- and y-directions, respectively.

3. Heat Transfer Analysis

Under usual boundary layer assumptions, the energy equation in the presence of thermal radiation effects is given by

$$u\frac{\partial T}{\partial x}+v\frac{\partial T}{\partial y}+w\frac{\partial T}{\partial z}=\alpha\frac{\partial^2 T}{\partial z^2}-\frac{1}{\rho C_p}\left(\frac{\partial q_\mathrm{r}}{\partial z}\right), \tag{13}$$

where T is the temperature, α is the thermal diffusivity, C_p is the specific heat at constant pressure, and q_r is the radiative heat flux. Using the Rosseland approximation for thermal radiation, the radiative heat flux is simplified as

$$q_\mathrm{r}=-\frac{4\sigma^*}{3k^*}\frac{\partial T^4}{\partial z}=-\frac{16\sigma^*}{3k^*}T^3\frac{\partial T}{\partial z}, \tag{14}$$

where σ^* and k^* are the Stefan–Boltzman constant and the mean absorption coefficient, respectively. Now (13) can be expressed as

$$\begin{aligned} &u\frac{\partial T}{\partial x}+v\frac{\partial T}{\partial y}+w\frac{\partial T}{\partial z}=\\ &\frac{\partial}{\partial z}\left[\left(\alpha+\frac{16\sigma^*T^3}{3\rho C_p k^*}\right)\frac{\partial T}{\partial z}\right]. \end{aligned} \tag{15}$$

It is important to note that in the previous studies on radiative heat transfer (see [31–42] and various references therein), T^4 in (14) was linearized through Taylor's series expansion about T_∞. However, we do not consider such approximation in the subsequent section to get more meaningful and practically useful results. Two kinds of thermal boundary conditions at the wall are considered and are treated separately in the following sections.

4. Constant Wall Temperature (CWT)

The boundary conditions in this case are

$$T=T_w\ \text{ at } z=0;\ \ T\to T_\infty\ \text{ as } z\to\infty, \tag{16}$$

with $T_w>T_\infty$ and T_w, T_∞ are the sheet's temperature and the ambient fluid's temperature, respectively.

Defining the non-dimensional temperature $\theta(\eta)=\frac{T-T_\infty}{T_w-T_\infty}$ and also $T=T_\infty(1+(\theta_w-1)\theta)$ with $\theta_w=\frac{T_w}{T_\infty}$ (temperature parameter), the first term on the right hand side of (14) can be written as $\alpha\frac{\partial}{\partial z}\left[\frac{\partial T}{\partial z}\left(1+R_d(1+(\theta_w-1)\theta)^3\right)\right]$, where $R_d=$

$\frac{16\sigma^* T_\infty^3}{3kk^*}$ denotes the radiation parameter, and $R_d = 0$ provides no thermal radiation effect. The last expression can be further simplified to

$$\frac{a(T_w - T_\infty)}{\Pr}\left[\left(1 + R_d\left(1 + (\theta_w - 1)\,\theta\right)^3\right)\theta'\right]', \tag{17}$$

where $\Pr = \frac{\nu}{\alpha}$ is the Prandtl number. Equation (15) becomes

$$\begin{aligned}&\frac{1}{\Pr}\left[\left(1 + R_d\left(1 + (\theta_w - 1)\,\theta\right)^3\right)\theta'\right]' \\ &+ (f + g)\,\theta' = 0,\end{aligned} \tag{18}$$

with the boundary conditions

$$\theta(0) = 1,\ \ \theta(+\infty) \to 0. \tag{19}$$

The heat transfer rate at the sheet is defined as

$$\begin{aligned}q_w &= -k\left(\frac{\partial T}{\partial z}\right)_{z=0} + (q_r)_w \\ &= -k\,(T_w - T_\infty)\sqrt{\frac{a}{\nu}}\left[1 + R_d\theta_w^3\right]\theta'(0),\end{aligned} \tag{20}$$

and with the help of the local Nusselt number $\mathrm{Nu}_x = \frac{x q_w}{k(T_w - T_\infty)}$, one obtains

$$\frac{\mathrm{Nu}_x}{\sqrt{\mathrm{Re}_x}} = -\left[1 + R_d\theta_w^3\right]\theta'(0). \tag{21}$$

5. Prescribed Surface Temperature (PST)

The boundary conditions in this case are (see Liu and Andersson [26])

$$\begin{aligned}&T = T_w = T_\infty + Ax^r y^s \ \text{ at } z = 0, \\ &T \to T_\infty \ \text{ as } z \to \infty,\end{aligned} \tag{22}$$

where $A > 0$ is a constant and the power indices r and s determine how the temperature at the sheet varies in the xy-plane. Now (15) (with linearized Rosseland approximation) reduces to

$$\frac{1 + R_d}{\Pr}\theta'' + (f + g)\,\theta' - (rf' + sg')\theta = 0, \tag{23}$$

with the following boundary conditions:

$$\theta(0) = 1,\ \ \theta(\infty) \to 0. \tag{24}$$

Here the surface heat flux becomes

$$\begin{aligned}q_w &= -k\left(\frac{\partial T}{\partial z}\right)_{z=0} + (q_r)_w \\ &= -kAx^r y^s\sqrt{\frac{a}{\nu}}\left[1 + R_d\right]\theta'(0),\end{aligned} \tag{25}$$

and using the definition of Nusselt number, one obtains

$$\frac{\mathrm{Nu}_x}{\sqrt{\mathrm{Re}_x}} = -\left[1 + R_d\right]\theta'(0). \tag{26}$$

6. Numerical Method

The dimensionless momentum equations (6)–(7) and the energy (18) and (23) with the relevant boundary conditions have been solved numerically by shooting method using fourth-order Runge–Kutta integration technique. For this purpose, we transform the original differential equations into a system of several first-order ordinary differential equations (ODEs), that is,

$$\begin{aligned}&\frac{\mathrm{d}f}{\mathrm{d}\eta} = F_1, \\ &\frac{\mathrm{d}F_1}{\mathrm{d}\eta} = F_2, \\ &\frac{\mathrm{d}F_2}{\mathrm{d}\eta} = F_1^2 + MF_1 - (f + g)\,F_2, \\ &\frac{\mathrm{d}g}{\mathrm{d}\eta} = G_1, \\ &\frac{\mathrm{d}G_1}{\mathrm{d}\eta} = G_2, \\ &\frac{\mathrm{d}G_2}{\mathrm{d}\eta} = G_1^2 + MG_1 - (f + g)\,G_2,\end{aligned} \tag{27}$$

with boundary conditions

$$\begin{aligned}&f(0) = 0,\ \ F_1(0) = 1,\ \ F_1(\infty) \to 0, \\ &g(0) = 0,\ \ G_1(0) = c,\ \ G_1(\infty) \to 0.\end{aligned} \tag{28}$$

CWT case:

$$\begin{aligned}&\frac{\mathrm{d}\theta}{\mathrm{d}\eta} = P, \\ &\frac{\mathrm{d}P}{\mathrm{d}\eta} = \\ &\frac{-\Pr(f + g)\,P - 3R_d P^2(\theta_w - 1)(1 + (\theta_w - 1)\theta)^2}{1 + R_d\left(1 + (\theta_w - 1)\theta\right)^3}.\end{aligned} \tag{29}$$

PST case:

$$\frac{d\theta}{d\eta} = P,$$
$$\frac{dP}{d\eta} = \frac{\Pr(\theta(rF_1 + sG_1) - (f+g)P)}{1+R_d}, \tag{30}$$

with boundary conditions

$$\theta(0) = 1, \quad \theta(\infty) \to 0. \tag{31}$$

Furthermore, because Runge–Kutta is an initial value solver whereas in current problem one of the boundary condition is given at infinity, suitable values of $f''(0)$, $g''(0)$, and $\theta'(0)$ are chosen and then numerical integration is carried out. We compare the calculated values for f', g', and θ at $\eta = 10$ (say) with the given boundary condition $f'(10) = 0$, $g'(10) = 0$, and $\theta(10) = 0$ and adjust the estimated values $f''(0)$, $g''(0)$, and $\theta'(0)$ to get a better approximation for the solution. Different values of η (such as $\eta = 10, 11, 12, 13$ etc.) are taken in our numerical computations so that numerical values are independent of η chosen. For the validation of the numerical method, the solutions are also obtained via the built in boundary value problem solver bvp4c of the software MATLAB.

The influence of embedding parameters on the velocity and temperature functions is described through graphical and numerical results. Figures 2 and 3 show the effects of magnetic field on the dimensionless x- and y-components of the velocity for different values of the velocity ratio c. The generalized uni-directional stretching wall problem can be recovered by choosing $c = 0$. On the other hand $c = 1$ corresponds to the axisymmetric flow due to a stretching sheet. The magnetic parameter M has a significant impact on the solutions. The presence of a magnetic field restricts the fluid motion and as a consequence the velocity decreases. With a gradual increase in M, the Lorentz force associated with the magnetic field increases and it produces more resistance to the transport phenomena. Irrespective of the value of magnetic parameter M, the velocity field f' and the boundary layer thickness are decreasing functions of the velocity ratio c. Figure 4 indicates that shear stress in both x-and y-directions increase with an increase in velocity ratio c. As a result the entrainment velocity $f(\infty) + g(\infty)$ is also an increasing function of c.

Figures 5 and 6 display the behaviour of radiation parameter R_d on the temperature θ in both CWT and PST cases, respectively. The results are shown for different values of c. It is observed that the temperature θ decreases with an increase in c in both cases of CWT and PST. In contrast to the linearized Rosseland approximation considered in previous studies [31 – 42], the radiation parameter in the present study has a significant role on the thermal boundary layer as can be seen from Figure 5. As expected the temperature and the thermal boundary layer thickness are increasing functions of R_d. Further the heat transfer rate at the sheet drastically decreases with an increase in R_d as the profiles become less steeper near the sheet as the radiation parameter increases. The Prandtl number is defined as the ratio of momentum diffusivity to the thermal diffusivity. It can be used to increase the rate of cooling in conducting flows. Temperature profiles for

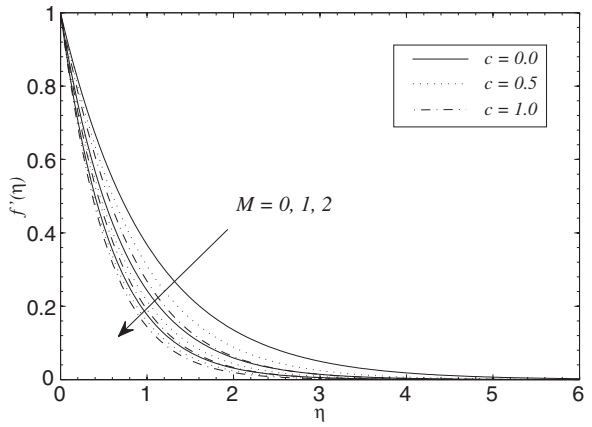

Fig. 2. Influence of magnetic parameter M and stretching ratio c on the velocity field $f'(\eta)$.

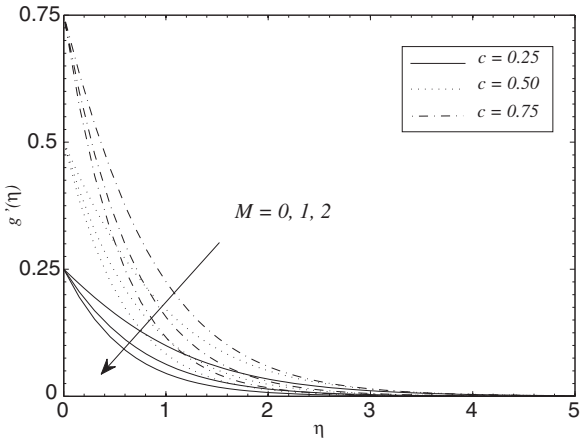

Fig. 3. Influence of magnetic parameter M and stretching ratio c on the velocity field $g'(\eta)$.

different values of Pr in both CWT and PST cases have been shown in Figures 7 and 8, respectively. Specifically, Prandtl number Pr = 0.72, 1.0, and 7.0 correspond to air, electrolyte solution such as salt water, and water, respectively. The results are shown for $R_d = 0$ and $R_d = 1$. Figure 7 indicates that the temperature θ and the thermal boundary layer thickness decrease with an increase in Pr. This is due to the fact that larger Prandtl number has a relatively lower thermal diffusivity which decreases conduction and thereby increases variation in the thermal characteristics. As expected the thermal penetration is limited for the fluids with larger Prandtl number when compared with the small Prandtl number fluids. In this work, the variation in the temperature θ with an increase in Pr is larger than that of previously reported works with the linearized Rosseland approximation.

Figures 9 and 10 compare the results of linear and nonlinear radiation for different values of R_d when $\theta_w = 1.1$ and $\theta_w = 3$, respectively. It is seen that linear and nonlinear results match each other better at $\theta_w = 1.1$ when compared with $\theta_w = 3$. The profiles show a significant deviation as the radiation parameter is gradually increased. Thus it can be concluded that linear and nonlinear radiation results match up smoothly when θ_w is close to one (say $\theta_w = 1.1$) and R_d is sufficiently small (say $R_d < 0.5$). Figure 11 plots the wall temperature gradient versus θ_w for different

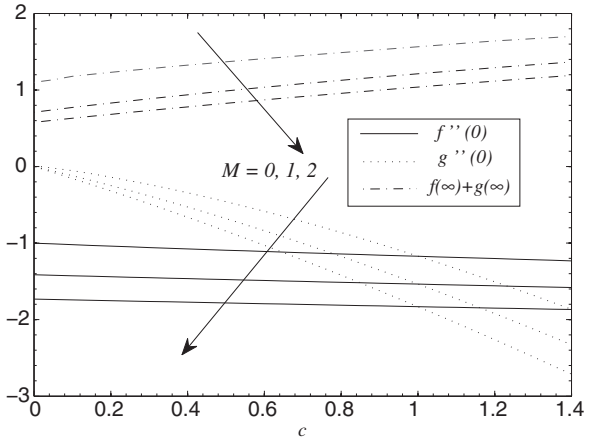

Fig. 4. Influence of magnetic parameter M and stretching ratio c on local skin friction coefficients and external velocity.

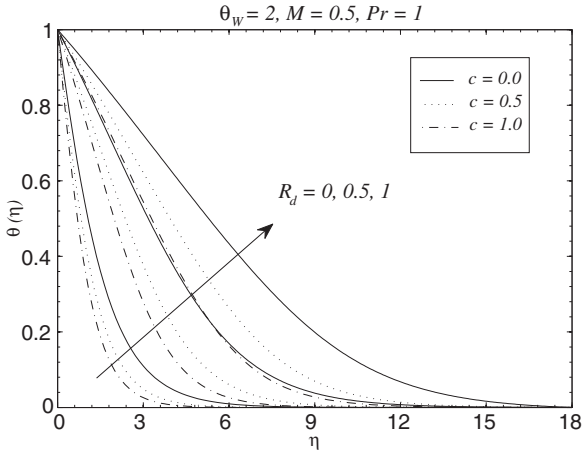

Fig. 5. Influence of radiation parameter R_d and stretching ratio c on temperature field $\theta(\eta)$ for the CWT case.

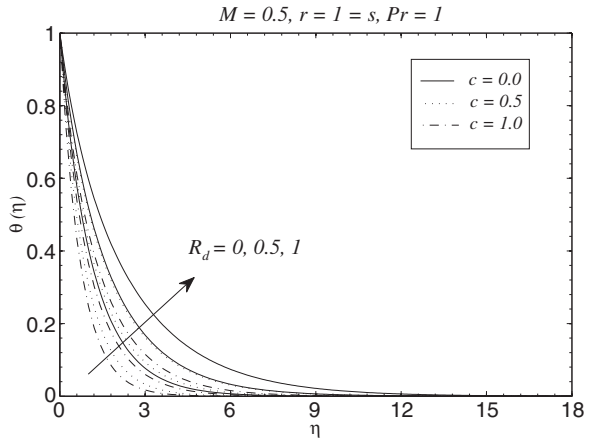

Fig. 6. Influence of radiation parameter R_d and stretching ratio c on temperature field $\theta(\eta)$ for the PST case.

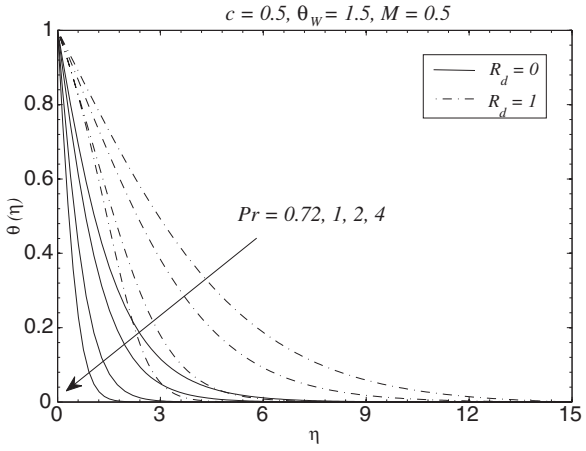

Fig. 7. Influence of radiation parameter R_d and Prandtl number Pr on temperature field $\theta(\eta)$ for the CWT case.

values of radiation parameter R_d. When $\theta_w \approx 1$, θ'' tends to a constant value for sufficiently smaller values of $R_d \approx 0.01$ which is in accordance with Cortell [45].

Table 1 shows the comparison of present solutions for $f''(0)$ and $g''(0)$ with those reported by Wang [22] and Liu and Andersson [26] whereas Table 2 presents a comparison of values $\theta'(0)$ for the PST case with results reported by Liu and Andersson [26] for various values of dimensionless power indices r and s. The present results are found in excellent agreement with those provided in [22] and [26]. We have also noticed that $|\theta'(0)|$ increases with an increase in the values of indices r and s. This observation leads to the conclusion that the heat transfer rate at the sheet can be increased by increasing the variation of wall temperature along the x- and y-directions. The numerical values of local Nusselt number $|\theta'(0)|$ for CWT and PST cases are given for various parametric values in Table 3. It is noticeable that the wall temperature gradient approaches the zero value as θ_w is increased indicating the existence of a point of inflection for the temperature distribution. This outcome is consistent with the findings obtained for two-dimensional flow [43]. Irrespective of magnetic parameter M, we observe a significant increase in the local Nusselt number as the thermal radiation effect intensifies. We noticed earlier in the graphical results that temperature profiles become increasingly steeper as Pr increases. As a result the Nusselt number, being pro-

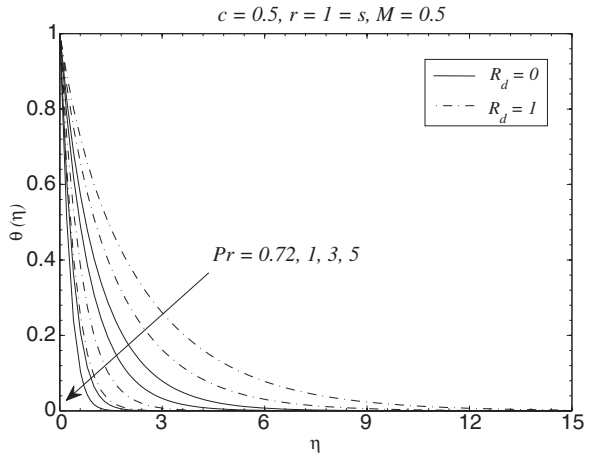

Fig. 8. Influence of radiation parameter R_d and Prandtl number Pr on temperature field $\theta(\eta)$ for the PST case.

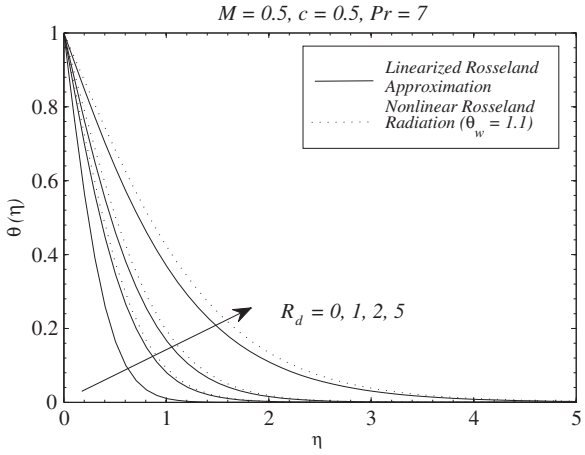

Fig. 9. Effects of thermal radiation on the temperature distribution through both linear and nonlinear radiative heat fluxes when $\theta_w = 1.1$ for the CWT case.

c	Present solution		Wang [22]		Liu and Andersson [26]	
	$f''(0)$	$g''(0)$	$f''(0)$	$g''(0)$	$f''(0)$	$g''(0)$
0.00	−1	0	−1	0	−1	0
0.25	−1.048811	−0.194564	−1.048813	−0.194564	−1.048813	−0.194565
0.50	−1.093095	−0.465205	−1.093097	−0.465205	−1.093096	−0.465206
0.75	−1.134486	−0.794618	−1.134485	−0.794622	−1.134486	−0.794619
1.00	−1.173721	−1.173721	−1.173720	−1.173720	−1.173721	−0.173721

Table 1. Numerical values of $f''(0)$ and $g''(0)$ with the previous studies for $M = 0$.

c		$r = 0$, $s = 0$	$r = -2$, $s = 0$	$r = 2$, $s = 0$	$r = 0$, $s = -2$	$r = 0$, $s = 2$
0.25	Present	−0.665928	0.554561	−1.364891	−0.413101	−0.883122
	Liu and Andersson [26]	−0.665933	0.554512	−1.364890	−0.413111	−0.883125
0.50	Present	−0.735333	0.308587	−1.395357	−0.263377	−1.106490
	Liu and Andersson [26]	−0.735334	0.308578	−1.395356	−0.263381	−1.106491
0.75	Present	−0.796472	0.135477	−1.425038	−0.126677	−1.292003
	Liu and Andersson [26]	−0.796472	0.135471	−1.425038	−0.126679	−1.292003

Table 2. Comparison of the heat transfer rate at the sheet $\theta'(0)$ with previous studies for the PST case when $M = 0 = R_d$, Pr = 1.

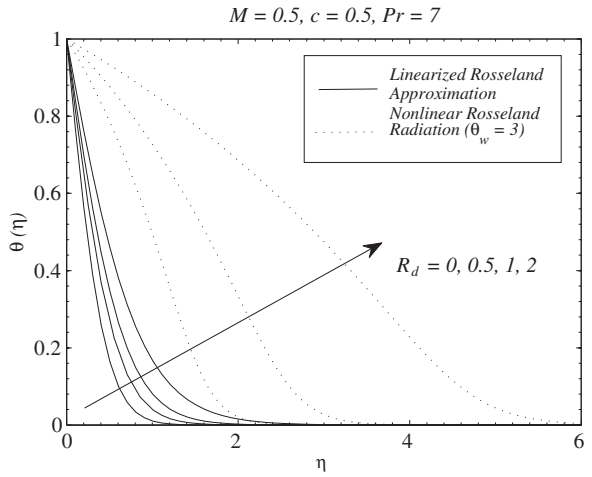

Fig. 10. Effects of thermal radiation on the temperature distribution through both linear and nonlinear radiative heat fluxes when $\theta_w = 3$ for the CWT case.

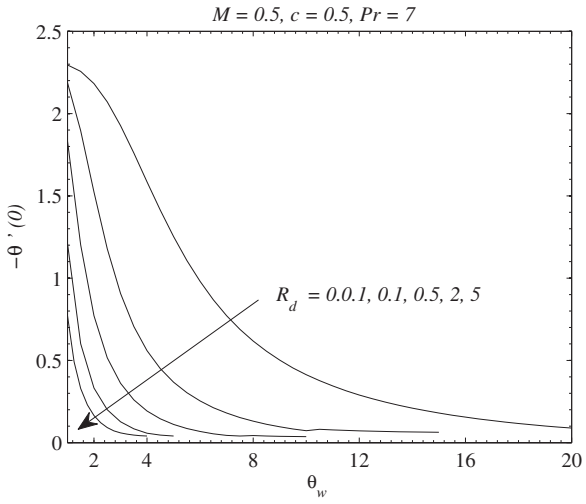

Fig. 11. Influence of temperature ratio parameter on wall heat transfer rate with the variation in radiation parameter.

Table 3. Heat transfer rate at the sheet $\theta'(0)$ for both CWT and PST cases when $c = 0.5$, $r = 2 = s$.

Pr	M	θ_w	R_d	$\theta'(0)$ CWT	PST
			0	−2.354383	−4.905743
	0	1	1	−1.593196	−3.386125
7		2	1	−0.547158	
			0	−2.267987	−4.803338
	1	1	1	−1.507175	−3.281324
		2	1	−0.499324	
			0	−0.547237	−1.307127
	0.5	1	1	−0.319122	−0.812635
0.72		2	1	−0.083342	
			0	−0.487439	−1.210997
	1.5	1	1	−0.274844	−0.726806
		2	1	−0.068696	

portional to the initial slope, increases with an increase in Pr in both CWT and PST case.

7. Concluding Remarks

MHD three-dimensional flow and heat transfer due to a bi-directional stretching sheet is investigated in presence of thermal radiation. For the heat transfer analysis two different heating processes, namely the constant wall temperature (CWT) and the prescribed surface temperature (PST), are taken into account. In this work the temperature function in the radiation term of energy equation (for the CWT case) is not further expanded about the ambient temperature. This results in a highly nonlinear but interesting energy equation which is governed by an additional temperature ratio parameter θ_w. The developed differential system is solved numerically through the shooting method with fifth-order Runge–Kutta integration technique. The key points of the present work may be summarized as follows:

(i) It is observed that the radiation parameter has a strong effect on the thermal boundary layer for any considered value of Prandtl number. The temperature θ and the thermal boundary layer thickness increase when the thermal radiation effect strengthens.

(ii) The temperature and the thermal boundary layer thickness are decreasing functions of Pr. This decrease accompanies with the larger rate of heat transfer at the bounding surface.

(iii) In the PST case, the dimensionless wall temperature gradient $|\theta'(0)|$ increases with an increase in dimensionless indices r and s. In other words, the heat transfer rate at the sheet can be increased by increasing the variation of wall temperature along the x- and y-directions.

(iv) The numerical results of $|\theta'(0)|$ are compared with those of Liu and Andersson [26] in the ab-

sence of thermal radiation effects and found in an excellent agreement.

(v) The current analysis for two-dimensional and axisymmetric flows can be obtained as special cases of the present study. To the best of our knowledge, this is the fundamental study of the application of nonlinear Rosseland approximation for thermal radiation in the three-dimensional boundary layer flow.

[1] H. Blasius, Z. Math. Phys. **56**, 1 (1908).
[2] B. C. Sakiadis, AIChE J. **7**, 26 (1961).
[3] L. J. Crane, J. Appl. Math. Phys. (ZAMP) **21**, 645 (1970).
[4] P. S. Gupta and A. S. Gupta, Can. J. Chem. Eng. **55**, 744 (1977).
[5] A. Chakrabarti and A. S. Gupta, Quart. Appl. Math. **37**, 73 (1979).
[6] L. J. Grubka and K. M. Bobba, ASME J. Heat Transf. **107**, 248 (1985).
[7] W. H. H. Banks, J. Méc. Theor. Appl. **2**, 375 (1983).
[8] C. K. Chen and M. I. Char, J. Math. Anal. Appl. **135**, 568 (1988).
[9] M. E. Ali, J. Heat Mass Transf. **16**, 280 (1995).
[10] I. Pop and T. Y. Na, Mech. Res. Comm. **25**, 263 (1998).
[11] E. Magyari and B. Keller, Eur. J. Mech. B-Fluids **19**, 109 (2000).
[12] S. J. Liao and I. Pop, Int. J. Heat Mass Transf. **47**, 75 (2004).
[13] M. Kumari and G. Nath, Commun. Nonlin. Sci. Numer. Simul. **14**, 3339 (2009).
[14] T. Hayat, M. Mustafa, and M. Sajid, Z. Naturforsch. **64a**, 827 (2009).
[15] T. Hayat, M. Mustafa, and S. Asghar, Nonlin. Anal.: Real World Appl. **11**, 3186 (2010).
[16] T. Hayat, M. Mustafa, and A. A. Hendi, Appl. Math. Mech.-Engl. **32**, 167 (2011).
[17] M. Mustafa, T. Hayat, and A. A. Hendi, ASME J. Appl. Mech. **79**, 021504 (2012).
[18] M. Mustafa, T. Hayat, and S. Obaidat, Z. Naturforsch. **67a**, 70 (2012).
[19] M. Ferdows, M. S Khan, M. M Alam, and S. Sun, Math. Probl. Eng. **3**, 2551 (2012).
[20] O. A. Beg, M. S Khan, I. Karim, M. M. Alam, and M. Ferdows, Appl. Nanosci. **1**, (2013), doi:10.1007/s13204-013-0275-0.
[21] M. S. Khan, I. Karim, and M. S. Islam, American Chem. Sci. J. **4**, 401 (2014).
[22] C. Y. Wang, Phys. Fluids **27**, 1915 (1984).
[23] K. N. Lakshmisha, S. Venkateswaran, and G. Nath, ASME J. Heat Transf. **110**, 590 (1988).
[24] H. Xu, S. J. Liao, and I. Pop, Eur. J. Mech. B **26**, 15 (2007).
[25] M. Sajid, T. Hayat, and I. Pop, Nonlin. Anal.: Real World Appl. **9**, 1811 (2008).
[26] I. C. Liu and H. I. Andersson, Int. J. Heat Mass Transf. **51**, 4018 (2008).
[27] T. Hayat, M. Qasim, and Z. Abbas, Commun. Nonlin. Sci. Numer. Simul. **15**, 2375 (2010).
[28] T. Hayat, M. Mustafa, and M. Sajid, Num. Meth. Part. Diff. Eq. **27**, 915 (2011).
[29] T. Hayat, M. Awais, A. Safdar, and A. A. Hendi, Nonlin. Anal.: Model. Cont. **17**, 47 (2012).
[30] I. C. Liu, H. H. Wang, and Y. F. Peng, Chem. Eng. Commun. **200**, 253 (2013).
[31] A. Raptis and C. Perdikis, J. Appl. Math. Phys. (ZAMP) **78**, 277 (1998).
[32] M. A. Seddeek, Int. J. Heat Mass Transf. **45**, 931 (2002).
[33] A. Raptis, C. Perdikis, and H. S. Takhar, Appl. Math. Comput. **153**, 645 (2004).
[34] R. C. Bataller, Appl. Math. Comput. **198**, 333 (2008).
[35] A. Ishak, Heat Mass Transf. **46**, 147 (2009).
[36] K. Bhattacharyya, Front. Chem. Sci. Eng. **5**, 376 (2011).
[37] S. Nadeem and R. U. Haq, J. Aerosp. Eng. doi:10.1061/(ASCE)AS.1943-5525.0000299 (2012).
[38] M. S. Khan, I. Karim, L. E. Ali, and I. Islam, Int. Nano Lett. **24**, 1 (2012).
[39] T. G. Motsumi and O. D. Makinde, Phys. Scr. **86**, 045003 (2012).
[40] M. S. Khan, I. Karim, and M. H. A. Biswas, Int. J. Basic Appl. Sci. **1**, 363 (2012).
[41] M. S. Khan, I. Karim, and M. H. A. Biswas, Acad. Res. Int. **3**, 80 (2012).
[42] M. S. Khan, M. M. Alam, and M. Ferdows, Procedia Eng. **56**, 316 (2013).
[43] A. Pantokratoras and T. Fang, Physic. Scr. **87**, 015703 (2013).
[44] A. Mushtaq, M. Mustafa, T. Hayat, and A. Alsaedi, J. Aerosp. Eng. **27**, (2014), doi:10.1061/(ASCE)AS.1943-5525.0000361.
[45] R. Cortell, J. King Saud Univ.-Sci. **26**, 161 (2014).
[46] A. Mushtaq, M. Mustafa, T. Hayat, and A. Alsaedi, J. Taiwan Inst. Chem. Eng. **45**, 1176 (2014).